Monatshefte für Chemie 136, 1715–1725 (2005)
DOI 10.1007/s00706-005-0359-y

**Monatshefte für Chemie**
**Chemical Monthly**
Printed in Austria

# The Effect of Ge, Ni, and Fe Doping on the Ga Activity in the CoGa B2 Phase

**Iwao Katayama**[1,*], **Adolf Mikula**[2], and **Toshio Oishi**[3]

[1] Dept. Materials and Manufacturing Science, Graduate School of Engineering,
Osaka University, 2-1 Yamadaoka, Suita, Osaka 565-0871, Japan
[2] Dept. Inorganic Chemistry–Materials Chemistry, University of Vienna,
A-1090 Vienna, Austria
[3] Faculty of Engineering, Dept. of Materials Sci. & Engineering,
Kansai University, 3-3-35 Yamate-cho, Suita, Osaka 564-8680, Japan

Received December 22, 2004; accepted March 28, 2005

**Summary.** Gallium activity in the B2 (CsCl-type) phase of ternary Co–Ga–$X$ ($X =$ Ge, Ni, and Fe) alloys was measured by the EMF method with a stabilized zirconia solid electrolyte. The temperature range was 1050–1250 K and the concentrations of the added elements were 2–6 at-% Ge and Ni, and 1–3 at-% Fe. The reference electrodes were Fe,$Fe_xO$ or Ga,$Ga_2O_3$. The effect on the activity of gallium in the B2 phase with the addition of other elements was found to be the largest with Ge and the smallest in the case of Ni.

**Keywords.** B2 phase; Cobalt–gallium–germanium; Cobalt–gallium–nickel; Cobalt–gallium–iron; Activity; Thermodynamics.

## Introduction

The Co–Ga system exhibits over a wide composition range an intermetallic compound with the cubic B2-(CsCl-type) structure [1, 2]. The change of the thermodynamic properties of Co–Ga, in the B2 phase through the addition of Ni, Ge, and Fe was measured. Ni and Fe atoms should go to the Co-sublattice and Ge to the Ga-sublattice. The defect structure of this ordered phase and the phase diagram have been studied by *Wunsch et al.* [2]. The physicochemical properties including thermodynamic data of this phase have attracted considerable interest in order to clarify the type of point defects. *Chang* and *Neumann* [3] used a theoretical model to calculate the defect concentration. They compiled the data of many B2 type phases and compared the experimental data with those obtained from modelling.

---

[*] Corresponding author. E-mail: katayama@mat.eng.osaka-u.ac.jp

For the Co–Ga B2 phase, vacancy and anti-structure concentration [2], activity [4, 5], vacancy and interaction energy [6, 7], and the enthalpy of formation [8, 9] have been determined. The influence of additional elements on the defect structure and/or thermodynamic properties was studied for the first time by *Jacobi et al.* [10] for Cu in the NiGa phase. For CoGa phase, the effect of Cu and Ni addition were studied by *Wachtel* and *Fleischmann* [11] and *Mikula et al.* [12], respectively.

The aim of this work is to study the effects of a small amount of an additional element (Ge, Ni, and Fe) on the activity of Ga in the CoGa phase by the EMF method with stabilized zirconia as a solid electrolyte between 1073 and 1273 K.

## Results and Discussion

The activity of gallium (the liquid gallium saturated with $Ga_2O_3$ is the reference state) was calculated from the EMF of the cell [I] by Eq. (1) where $E$ is the EMF of the cell, $F$ the Faraday constant, $R$ the gas constant, $T$ the temperature in K, and $a$ the activity of Ga.

$$(-)\mathrm{Ga,Ga_2O_3|ZrO_2(+Y_2O_3\ or\ CaO)|Ga\text{-}alloys,\ Ga_2O_3(+)} \qquad [\mathrm{I}]$$

$$-3EF = RT\ln a_{\mathrm{Ga}} \qquad (1)$$

When a reference electrode other than $Ga,Ga_2O_3$ is to be used (in this study, $Fe,Fe_xO$), the EMF of the following cell (II) has to be known, and the temperature dependence of this cell is given by Eq. (2).

$$(-)\mathrm{Pt,Re/Ga,Ga_2O_3|ZrO_2(+Y_2O_3)|Fe,Fe}_x\mathrm{O(+)} \qquad [\mathrm{II}]$$

$$E/\mathrm{mV} = 519.6 - 0.2322T/\mathrm{K} \pm 1.4 \qquad (2)$$

**Table 1.** Alloy composition of Co–Ga–Ge (mole fraction)

| Alloy | Co | Ga | Ge |
|---|---|---|---|
| 1 | 0.5651 | 0.4147 | 0.0202 |
| 2 | 0.5292 | 0.4508 | 0.0200 |
| 3 | 0.4900 | 0.4900 | 0.0200 |
| 4 | 0.4508 | 0.5292 | 0.0200 |
| 5 | 0.4116 | 0.5684 | 0.0200 |
| 6 | 0.5569 | 0.4032 | 0.0399 |
| 7 | 0.5184 | 0.4416 | 0.0400 |
| 8 | 0.4800 | 0.4800 | 0.0400 |
| 9 | 0.4416 | 0.5184 | 0.0400 |
| 10 | 0.4032 | 0.5568 | 0.0400 |
| 11 | 0.5452 | 0.3948 | 0.0600 |
| 12 | 0.5075 | 0.4324 | 0.0601 |
| 13 | 0.4700 | 0.4700 | 0.0600 |
| 14 | 0.4324 | 0.5076 | 0.0600 |
| 15 | 0.3948 | 0.5452 | 0.0600 |

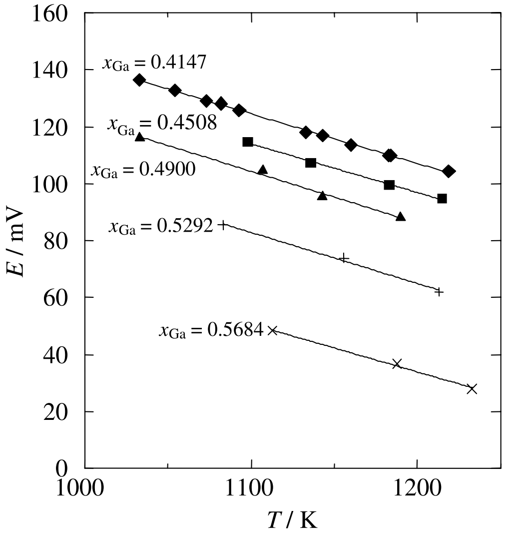

**Fig. 1a.** Temperature dependence of the EMF of the cell Ga,$Ga_2O_3$|$ZrO_2(+Y_2O_3)$|$Co_{1-x}Ga_xGe_{0.02}$, $Ga_2O_3$

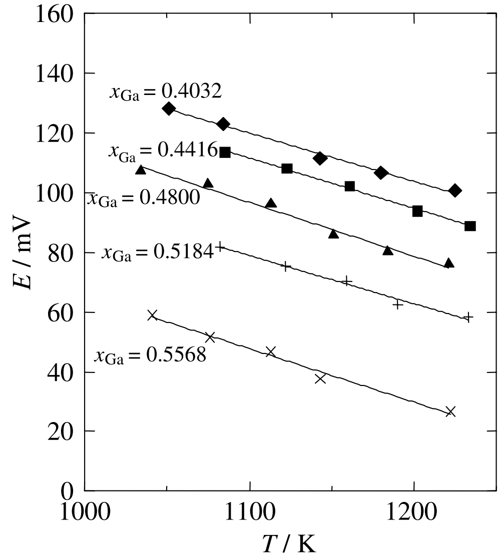

**Fig. 1b.** Temperature dependence of the EMF of the cell Ga,$Ga_2O_3$|$ZrO_2(+Y_2O_3)$|$Co_{1-x}Ga_xGe_{0.04}$, $Ga_2O_3$

The activity coefficient $\gamma$ of Ga is defined as the ratio of the activity of Ga to the mol fraction $x_{Ga}$. As the electric contact materials 'Kanthal, Re' was used for Ga,$Ga_2O_3$ and CoGa–Ge,$Ga_2O_3$ electrode and 'Pt-Re' was used for Ga,$Ga_2O_3$, and $(Co_{1-x}Ga_x)_{1-y}M_y$,$Ga_2O_3$ ($M$ = Ni and Fe).

## *Co–Ga–Ge Alloys*

The compositions of the alloys are shown in Table 1. The experimental results are given in Figs. 1a–1c. In Fig. 1a 2 at-% Ge were added to the Co–Ga alloys, in

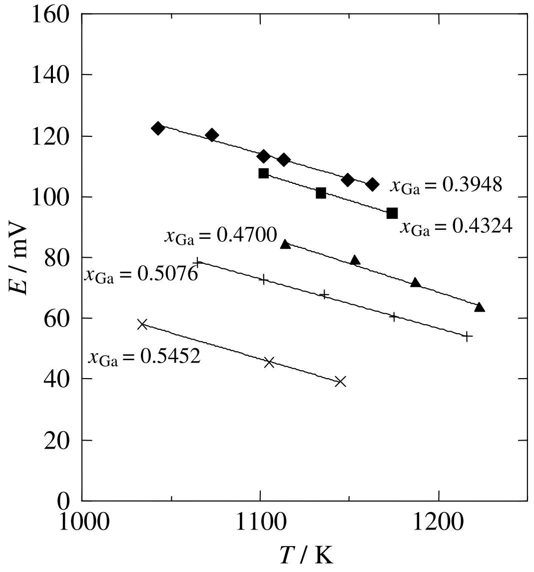

**Fig. 1c.** Temperature dependence of the EMF of the cell $Ga,Ga_2O_3|ZrO_2(+Y_2O_3)|Co_{1-x}Ga_xGe_{0.06}, Ga_2O_3$

**Table 2.** Temperature dependence of the EMF of cell (I) for Co–Ga–Ge alloys

| Alloy | $E$/mV | Temp. range/K | $x_{Ge}$ |
|---|---|---|---|
| 1 | 316.75–0.1747$T \pm$ 0.83 | 1033–1219 | |
| 2 | 302.00–0.1709$T \pm$ 0.48 | 1098–1215 | |
| 3 | 303.91–0.1814$T \pm$ 1.55 | 1033–1190 | 0.02 |
| 4 | 280.21–0.1794$T \pm$ 1.14 | 1083–1213 | |
| 5 | 235.96–0.1684$T \pm$ 0.75 | 1113–1233 | |
| 6 | 297.53–0.1615$T \pm$ 1.43 | 1051–1225 | |
| 7 | 296.89–0.1685$T \pm$ 0.87 | 1085–1234 | |
| 8 | 295.7–0.1809$T \pm$ 1.88 | 1034–1221 | 0.04 |
| 9 | 256.65–0.1616$T \pm$ 1.95 | 1082–1233 | |
| 10 | 245.27–0.1796$T \pm$ 2.46 | 1041–1222 | |
| 11 | 294.63–0.1641$T \pm$ 1.80 | 1043–1163 | |
| 12 | 306.66–0.1808$T \pm$ 0.45 | 1102–1174 | |
| 13 | 296.08–0.1896$T \pm$ 1.18 | 1114–1223 | 0.06 |
| 14 | 251.82–0.1626$T \pm$ 0.67 | 1065–1216 | |
| 15 | 234.35–0.1706$T \pm$ 0.34 | 1034–1145 | |

Fig. 1b 4 at-% Ge, and in Fig. 1c 6 at-% Ge. The relations between EMF ($E$/mV) and temperature ($T$/K) were obtained by a least-squares regression analysis, and the results are shown in Table 2. Activities of gallium at 1173 K are given in Table 3 and plotted in Fig. 2. We can see that the addition of germanium increases the activity of gallium over the whole composition range, except for 2 at-% Ge. There is a significant change in the activity of Ga in the region $x_{Ga} > 0.5$.

**Table 3.** Activity and activity coefficient of Ga at 1173 K in the Co–Ga–Ge alloys

| Alloy | $x_{Ga}$ | $a_{Ga}$ | $\gamma_{Ga}$ | Log $a_{Ga}$ |
|---|---|---|---|---|
| 1 | 0.4147 | 0.0362 | 0.0873 | −1.4413 |
| 2 | 0.4508 | 0.0491 | 0.1090 | −1.3089 |
| 3 | 0.4900 | 0.0669 | 0.1365 | −1.1746 |
| 4 | 0.5292 | 0.1261 | 0.2383 | −0.8993 |
| 5 | 0.5684 | 0.3197 | 0.5624 | −0.4953 |
| 6 | 0.4032 | 0.0404 | 0.1003 | −1.3936 |
| 7 | 0.4416 | 0.0526 | 0.1191 | −1.2790 |
| 8 | 0.4800 | 0.0904 | 0.1884 | −1.0438 |
| 9 | 0.5184 | 0.1365 | 0.2634 | −0.8649 |
| 10 | 0.5568 | 0.3581 | 0.6432 | −0.4460 |
| 11 | 0.3948 | 0.0482 | 0.1222 | −1.3170 |
| 12 | 0.4324 | 0.0604 | 0.1396 | −1.2190 |
| 13 | 0.4700 | 0.1123 | 0.2389 | −0.9496 |
| 14 | 0.5076 | 0.1631 | 0.3214 | −0.7875 |
| 15 | 0.5452 | 0.3620 | 0.6640 | −0.4413 |

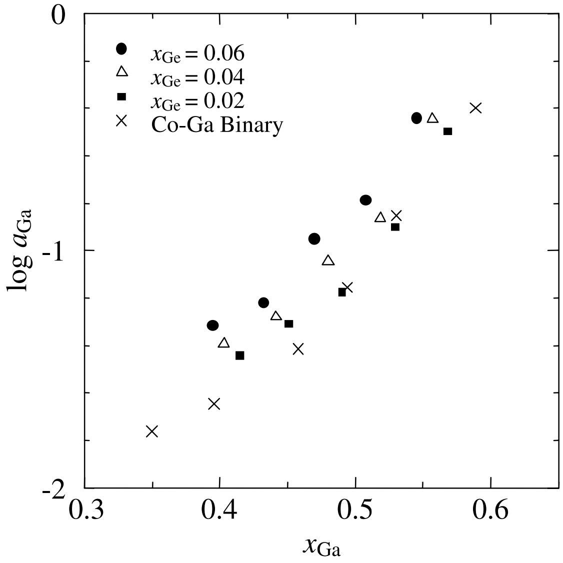

**Fig. 2.** Log of the activity of Ga *vs.* content of Ga in the Co–Ga–Ge alloys at 1173 K

### *Co–Ga–Ni Alloys*

The experimental data are shown in Figs. 3a–3c with Ni contents of 2 at-%, 4 at-%, and 6 at-%. The temperature dependence of the EMF of the cell with Fe,$Fe_xO$ as a reference electrode is shown in Table 4 and the calculated values with Ga,$Ga_2O_3$ as a reference electrode. The activity of Ga in the Co–Ga–Ni alloys at 1173 K is given in Table 5 and plotted in Fig. 4. In the Co-rich region

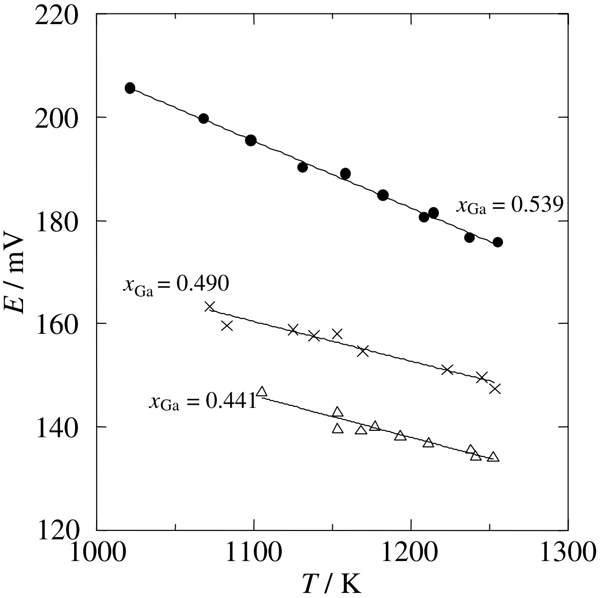

**Fig. 3a.** Temperature dependence of the EMF of the cell Fe,FeO|$ZrO_2(+Y_2O_3)$|$Co_{1-x}Ga_xNi_{0.02}$, $Ga_2O_3$

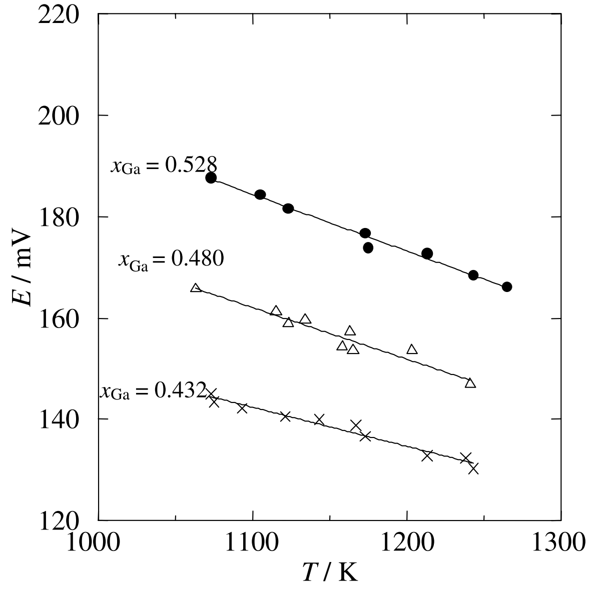

**Fig. 3b.** Temperature dependence of the EMF of the cell Fe,FeO|$ZrO_2(+Y_2O_3)$|$Co_{1-x}Ga_xNi_{0.04}$, $Ga_2O_3$

($x_{Ga}<0.5$) Ni addition increases $a_{Ga}$ independent of the amount of Ni. In the Ga-rich region the activity increases with increasing nickel content, 2 at-% Ni addition has no effect. At the Co-rich region ($x_{Ga}<0.5$) the addition of Ni

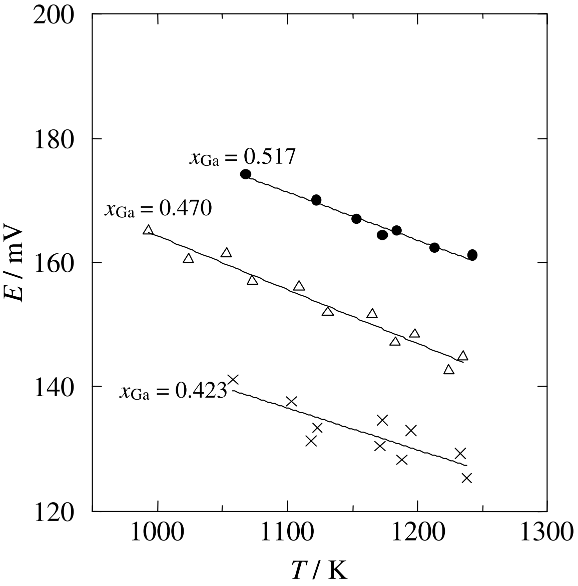

**Fig. 3c.** Temperature dependence of the EMF of the cell Fe,FeO|$ZrO_2(+Y_2O_3)$|$Co_{1-x}Ga_xNi_{0.06}$, $Ga_2O_3$

**Table 4.** Temperature dependence of the cell Ref. |$ZrO_2$(+CaO)|Co–Ga–Ni alloys, $Ga_2O_3$

| Alloy composition | | | No. | $E_1$/mV | $E$/mV | Temp. range/K |
|---|---|---|---|---|---|---|
| $x_{Co}$ | $x_{Ga}$ | $x_{Ni}$ | | Ref. = Fe,$Fe_xO$ | Ref. = Ga,$Ga_2O_3$ | |
| 0.539 | 0.441 | 0.02 | 1 | $235.1–0.0811T \pm 2.2$ | $284.5–0.1511T$ | 1105–1252 |
| 0.490 | 0.490 | 0.02 | 2 | $245.2–0.0771T \pm 2.1$ | $274.4–0.1551T$ | 1072–1253 |
| 0.441 | 0.539 | 0.02 | 3 | $338.1–0.1298T \pm 1.2$ | $181.5–0.1024T$ | 1021–1255 |
| 0.528 | 0.432 | 0.04 | 4 | $227.3–0.0772T \pm 1.6$ | $292.3–0.1550T$ | 1073–1243 |
| 0.480 | 0.480 | 0.04 | 5 | $274.1–0.1019T \pm 2.0$ | $245.5–0.1303T$ | 1063–1241 |
| 0.432 | 0.528 | 0.04 | 6 | $307.5–0.1119T \pm 2.2$ | $212.1–0.1203T$ | 1073–1265 |
| 0.512 | 0.423 | 0.06 | 7 | $210.7–0.0674T \pm 4.0$ | $308.9–0.1648T$ | 1058–1238 |
| 0.470 | 0.470 | 0.06 | 8 | $250.8–0.0865T \pm 2.3$ | $268.8–0.1457T$ | 993–1235 |
| 0.423 | 0.517 | 0.06 | 9 | $256.4–0.0773T \pm 1.3$ | $263.2–0.1549T$ | 1068–1242 |

**Table 5.** Activity of Ga in Co–Ga–Ni alloys at 1173 K

| No. | $x_{Ga}$ | $a_{Ga}$ | Log $a_{Ga}$ | $\gamma_{Ga}$ |
|---|---|---|---|---|
| 1 | 0.441 | 0.041 | −1.3825 | 0.094 |
| 2 | 0.490 | 0.064 | −1.1919 | 0.131 |
| 3 | 0.539 | 0.162 | −0.7912 | 0.300 |
| 4 | 0.432 | 0.038 | −1.4241 | 0.087 |
| 5 | 0.480 | 0.064 | −1.1943 | 0.133 |
| 6 | 0.528 | 0.122 | −0.9150 | 0.230 |
| 7 | 0.423 | 0.032 | −1.4899 | 0.077 |
| 8 | 0.470 | 0.055 | −1.2618 | 0.116 |
| 9 | 0.517 | 0.089 | −1.0505 | 0.172 |

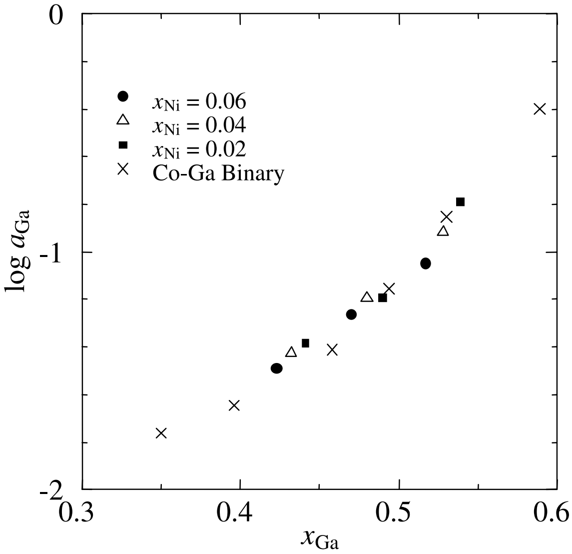

**Fig. 4.** Log of the activity of Ga *vs.* content of Ga in the Co–Ga–Ni alloys at 1173 K

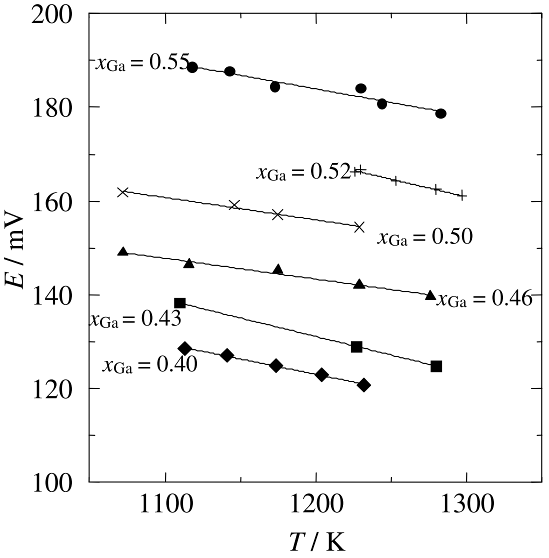

**Fig. 5a.** Temperature dependence of the EMF of the cell Fe,FeO|$ZrO_2(+Y_2O_3)$|$Co_{1-x}Ga_xFe_{0.01}$, $Ga_2O_3$

increases the activity of Ga only slightly and in the Ga-rich region the addition of Ni has nearly no effect.

### *Co–Ga–Fe Alloys*

The experimental results after the addition of 1 at-% Fe and 3 at-% Fe are shown in Figs. 5a–5b and Tables 6 and 7. In Fig. 6 the log $a_{Ga}$ is plotted *versus* the Ga

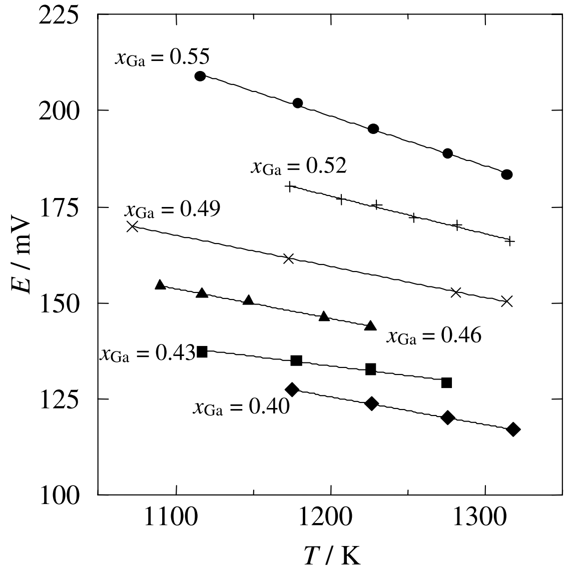

**Fig. 5b.** Temperature dependence of the EMF of the cell Fe,FeO|$ZrO_2(+Y_2O_3)$|$Co_{1-x}Ga_xFe_{0.03}$, $Ga_2O_3$

**Table 6.** Temperature dependence of cell Ref. |$ZrO_2$(+CaO)|Ga–Ga–Fe alloys, $Ga_2O_3$

| Alloy composition | | | No. | $E_1$/mV | $E$/mV | Temp. range/K |
|---|---|---|---|---|---|---|
| $x_{Co}$ | $x_{Ga}$ | $x_{Fe}$ | | Ref. = Fe,$Fe_xO$ | Ref. = Ga,$Ga_2O_3$ | |
| 0.59 | 0.40 | 0.01 | 1 | $201.5-0.0654T \pm 0.3$ | $318.1-0.1668T$ | 1113–1232 |
| 0.56 | 0.43 | 0.01 | 2 | $225.8-0.0789T \pm 0.8$ | $293.8-0.1533T$ | 1110–1280 |
| 0.53 | 0.46 | 0.01 | 3 | $196.5-0.0443T \pm 0.6$ | $321.1-0.1879T$ | 1072–1276 |
| 0.49 | 0.50 | 0.01 | 4 | $213.1-0.0476T \pm 0.6$ | $306.5-0.1846T$ | 1072–1229 |
| 0.47 | 0.52 | 0.01 | 5 | $258.9-0.0754T \pm 0.4$ | $260.7-0.1568T$ | 1226–1297 |
| 0.44 | 0.55 | 0.01 | 6 | $253.4-0.0579T \pm 6.6$ | $266.2-0.1743T$ | 1118–1283 |
| 0.57 | 0.40 | 0.03 | 7 | $212.7-0.0726T \pm 0.3$ | $306.9-0.1596T$ | 1175–1318 |
| 0.54 | 0.43 | 0.03 | 8 | $193.6-0.0500T \pm 0.8$ | $326.0-0.1822T$ | 1117–1275 |
| 0.51 | 0.46 | 0.03 | 9 | $238.8-0.0774T \pm 0.2$ | $280.8-0.1548T$ | 1090–1226 |
| 0.48 | 0.49 | 0.03 | 10 | $256.9-0.0812T \pm 1.1$ | $262.7-0.1510T$ | 1072–1314 |
| 0.45 | 0.52 | 0.03 | 11 | $295.5-0.0981T \pm 0.5$ | $224.1-0.1341T$ | 1174–1316 |
| 0.42 | 0.55 | 0.03 | 12 | $354.0-0.1295T \pm 0.6$ | $165.6-0.1027T$ | 1116–1314 |

content at 1173 K. At 1 at-% Fe the activity of gallium increases in the Co-rich region but decreases in the Ga-rich region. At 3 at-% Fe the activity of gallium is higher over the whole composition range. The results correspond to the study of *Whittle et al.* [16] for the vacancy concentration and site occupancy, by X-ray and bulk density measurements, and *Mössbauer* spectroscopy. With increasing Fe content the vacancy concentration increases sharply.

**Table 7.** Activity of Ga in Co–Ga–Fe alloys at 1173 K

| No. | $x_{Ga}$ | $a_{Ga}$ | $\gamma_{Ga}$ | Log $a_{Ga}$ |
|---|---|---|---|---|
| 1 | 0.40 | 0.0264 | 0.0660 | −1.578 |
| 2 | 0.43 | 0.0340 | 0.0790 | −1.469 |
| 3 | 0.46 | 0.0504 | 0.1095 | −1.298 |
| 4 | 0.50 | 0.0692 | 0.1385 | −1.160 |
| 5 | 0.52 | 0.1024 | 0.1970 | −0.990 |
| 6 | 0.55 | 0.1600 | 0.2909 | −0.796 |
| 7 | 0.40 | 0.0287 | 0.0716 | −1.543 |
| 8 | 0.43 | 0.0357 | 0.0830 | −1.447 |
| 9 | 0.46 | 0.0526 | 0.1144 | −1.279 |
| 10 | 0.49 | 0.0789 | 0.1610 | −1.103 |
| 11 | 0.52 | 0.1377 | 0.2648 | −0.861 |
| 12 | 0.55 | 0.2620 | 0.4763 | −0.582 |

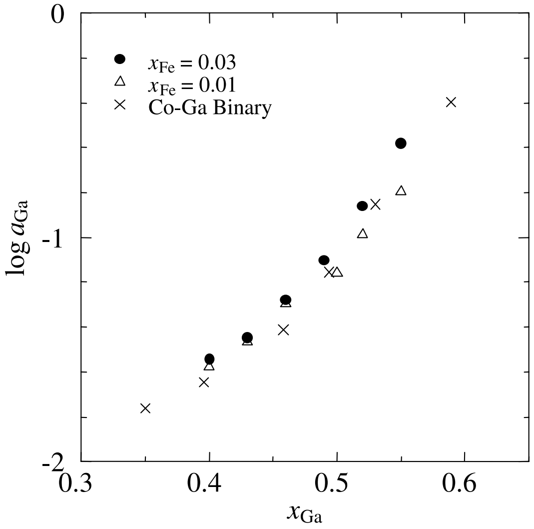

**Fig. 6.** Log of the activity of Ga *vs.* content of Ga in the Co–Ga–Fe alloys at 1173 K

## Materials and Experimental Procedure

The materials used in the preparation of the alloys were Ga and Ge (99.9999 wt-% purity), Co (99.9%), and Ni (99.99%). The alloys $(Co_{1-x}Ga_x)_{1-y}M_y$ [$M$ = Ge, Ni, and Fe] were prepared by heating the elements with the desired compositions up to 1523 or 1573 K in a stabilized zirconia crucible held under $H_2$-atmosphere in an alumina reaction tube. The alloys were shielded in evacuated quartz ampoules and homogenized at about 1200 K for longer than 10 days. After this the alloys were grinded to a powder by a diamond dental drill. $Ga_2O_3$ powder (99.99 mass-% purity) was added to produce the alloy electrode (7:1 in a mass ratio), followed by a heat treatment at the measuring temperatures of the EMF in an evacuated silica ampoule for about 2 days.

A stabilized zirconia crucible with a round bottom ($0.92\ ZrO_2 + 0.08\ Y_2O_3$, and $0.89\ ZrO_2 + 0.11\ CaO$), size $8^{od} \times 5^{id} \times 50^{length}$ mm, produced at Nikkato Co. Ltd was used as a solid electrolyte. Fe,$Fe_xO$ or Ga,$Ga_2O_3$ were used as the reference electrode. Cell apparatus and experimental procedure were quite similar to those used in the investigations of Cu–In [13], Pd–Ga [14], and CoGa–Sb [15]. A spring was inserted between lower and upper alumina tubes on the electrode to keep good contact between the alloy electrode and the electrolyte. The reaction tube was evacuated and filled with purified argon gas at rt. The inner part of the reaction tube was kept at a pressure higher than 1 atm of Ar gas. For each ternary alloy the temperature range of the EMF measurements was slightly different. The CoGa–Ge was measured between 1033–1234 K, the CoGa–Ni at 993–1265 K, and the CoGa–Fe at 1073–1318 K on 15, 9, and 12 alloys, respectively. The homogeneity of the samples was checked by powder X-ray diffraction, all samples were found to be single phase with the cubic B2-(CsCl-type) structure.

## Conclusion

Gallium activity in the B2 phase regions of Co–Ga–$M$ ($M$ = Ge, Ni, and Fe) systems was measured by the EMF method with a stabilized zirconia solid electrolyte between 1073 and 1273 K. The effect of the additional elements on the activity of gallium is most pronounced in case of Ge, and smallest in case of Ni.

## Acknowledgement

This research was partially supported by Grand-in-Aid for Scientific Research (C2-1455072) of the Japan Society for the Promotion of Science.

## References

[1] Elliott RP (1965) Constitution of Binary Alloys, First Supplement. McGraw-Hill, New York, p 320
[2] Wunsch KM, Wachtel E (1982) Z Metallkd **73**: 311
[3] Chang YA, Neumann JP (1982 ) Prog Solid State Chem **14**: 221; (1979) Z Metallkd **70**: 118
[4] Katayama I, Kemori N, Kozuka Z (1975) Trans JIM **16**: 423
[5] Mikula A, Chang YA, Neumann JP (1978) Trans JIM **19**: 307
[6] Van Ommen AH, Waegemaekers AAHJ, Moleman AC, Schlatter H, Bakker H (1981) Acta Metall **29**: 123
[7] Waegemaekers AAHJ, van Ommen AH (1982) J Phys F Met Phys **12**: 2829
[8] Henig E-T, Lukas H (1997) Symp on Thermal Analysis and Calorimet. Plymouth, UK; Henig E-T, Lukas HL, Petzow G (1982) Z Metallkd **73**: 87
[9] Predel B, Vogelbein W (1975) Thermochim Acta **13**: 133
[10] Jacobi H, Stoeckel D, Lukas HL (1971) Z Metallkd **62**: 305
[11] Wachtel E, Fleischmann O (1976) Z Metallkd **67**: 744
[12] Mikula A, Schuster W, Chang YA, Henig E-T (1987) Z Metallkd **78**: 172
[13] Katayama I, Miyakusu K, Iida T (2002) J Min Metall Sec (Yugo) **38b**: 23
[14] Katayama I, Hattori Y, Iida T (2002) Proc. Internat Conf on Designing of Interfacial Structures in Advanced Materials and Their Joints, 26–28 Nov 2002, p 484
[15] Katayama I, Tadashi M, Oishi T (2003) Intermetallics **11**: 1161
[16] Whittle GL, Clark PE, Cywinski R (1980) J Phys F: Metal Phys **10**: 2093